A Report

entitled

ANALYTICAL STUDY OF TWIN-JET SHIELDING TWO-DIMENSIONAL MODEL

NASA Grant No. NAG 1-11

Submitted by the

TEXAS A & M RESEARCH FOUNDATION

to

National Aeronautics and Space Administration
Langely Research Center

Prepared by

Dr. Carl H. Gerhold

of the

Department of Mechanical Engineering
Texas A & M University
College Station, Texas 77843

August 15, 1980

TABLE OF CONTENTS

ANALYTICAL STUDY OF TWIN JET SHIELDING - TWO-DIMENSIONAL MODEL

I INTRODUCTION

One of the drawbacks of the growing dependence on air travel is the increased impact of aircraft noise. Reduction of this impact through noise control requires identification of the mechanisms of aircraft generated noise. Noise estimation includes consideration not only of the noise sources on the aircraft, but also of the propagation path between the source and the receiver. One of the factors affecting the noise transmission path is shielding of one jet by another. The shielding jet, because of the high temperature and flow speed with respect to the immediate surroundings, acts as a partial barrier between the shielded jet and the receiver. The resultant alteration of the propagation path not only affects the overall aircraft noise level, but also indicates the possibility of jet engine installation as a means of aircraft noise control.

It is the purpose of this paper to discuss the development of the analytical model to estimate the shielding of one jet by an adjacent jet in a twin jet configuration.

The problem of reflection and transmission of sound by a moving medium has been addressed assuming a plane wave incident on a plane interface (1,2,3,4). In such models, the redistribution of the incident sound is estimated along the axis of the jet.

In the present study, the azimuthal redistribution of sound, defining the shadow zone is investigated. The wave equations are solved in the plane normal to the jet axis. Thus, the noise source considered is essentially a line source. It is assumed to emit at discrete frequency and is at rest with respect to the shielding jet. The shielding jet is assumed to be a cylinder of heated flow in which the temperature is constant across the jet.

II FORMULATION OF THE MODEL

The mechanisms by which shielding occurs are reflection and refraction of sound at the boundary between the jet and the surrounding air and by diffraction around the jet.

The noise source is a stationary, discrete-frequency source located at S, Θ_o ; radiating into the plane normal to the shielding jet axis. The shielding jet, of radius a, is centered on the origin. The temperature profile is assumed to be uniform across the cross-section of the jet. The model is illustrated in Figure 1.

The expressions for acoustic velocity potential are written for the two regions: region I surrounding the shielding jet, and region II within the jet.

Region I

a) Incident upon the cylinder, emitted from source

$$\nabla^2 \phi - \frac{1}{c_o^2} \phi = Q_0 e^{-i\omega t} \delta(r-S)\ \delta(\Theta-\Theta_o) \qquad 1a)$$

b) reflected from cylinder

$$\nabla^2 \phi - \frac{1}{c_o^2} \phi = o \qquad 1b)$$

Region II (within shielding jet)

$$\nabla^2 \phi - \frac{1}{c_1^2} \phi = o \qquad 2)$$

where:

c_o = sound speed in the surrounding medium

Q_o = source strength

ω = radial frequency of source emission

δ = Dirac delta function

c_1 = sound speed within a shielding jet

$$\nabla^2 = \frac{\partial^2}{\partial r^2} + \frac{1}{r}\frac{\partial}{\partial r} + \frac{1}{r^2}\frac{\partial^2}{\partial \Theta^2}$$

At the interface between the surrounding medium and the jet, the following boundary conditions must be met.

1) Pressure continuity

$$-\rho_0 \left.\frac{\partial \Phi}{\partial t}\right|_0 = -\rho_1 \left.\frac{\partial \Phi}{\partial t}\right|_1 \quad \text{at } r=a \qquad 3a)$$

2) Normal velocity continuity

$$\left.\frac{\partial \Phi}{\partial r}\right|_0 = \left.\frac{\partial \Psi}{\partial r}\right|_1 \quad \text{at } r=a \qquad 3b)$$

The solution of the wave equation in two dimensions for a source located at coordinates S, Θ_0 is shown in reference 5, chapter 7 . Thus the solution of equation 1a), describing the wave incident on the jet is:

$$\Phi_{in} = \frac{-iQ_0 e^{-i\omega t}}{4} \sum_{m=0}^{\infty} \varepsilon_m \cos m(\Theta-\Theta_0) \begin{cases} J_m(k_0 r) H_m(k_0 S) & r<S \\ H_m(k_0 r) J_m(k_0 S) & r>S \end{cases} \qquad 4a$$

where : $\varepsilon_m = \begin{cases} 1 & m=0 \\ 2 & m\neq 0 \end{cases}$

J_m = Bessel Function of the first kind of order m

H_m = Hankel Function of the first kind $= J_m + i\,Y_m$

Y_m = Modified Bessel Function of the first kind of order m

k_0 = wave number $= \omega/c_0$

$i = \sqrt{-1}$

The solution of the homogeneous wave equation, in region I, for the wave scattered from the jet is:

$$\Phi_{sc} = e^{-i\omega t} \sum_{m=o}^{\infty} A_m \cos m\,(\theta-\theta_0)\, H_m(k_0 r) \qquad 4b)$$

where the Hankel Function is chosen to ensure that the wave is outgoing.

The solution of the wave equation for the wave transmitted into the jet is:

$$\Phi_{tr} = e^{-i\omega t} \sum_{m=o}^{\infty} B_m \cos m(\theta-\theta_0)\, J_m(k_1 r) \qquad 4c)$$

where: $k_1 = \omega/c_1$

The Bessel Function is chosen because the acoustic velocity potential must be finite at the origin.

Applying the boundary conditions:

1. Pressure continuity

$$-\rho_0 \left(\frac{\partial \Phi_{in}}{\partial t} + \frac{\partial \Phi_{sc}}{\partial t} \right) = -\rho_1 \frac{\partial \Phi_{tr}}{\partial t} \quad \text{at } r=a \qquad 5a)$$

$$\rho_0 \left(\frac{iQ_0}{4} \sum_{m=o}^{\infty} \varepsilon_m \cos m(\theta-\theta_0)\, J_m(k_0 a) H_m(k_0 S) \right.$$

$$\left. - \sum_{m=o}^{\infty} A_m \cos m(\theta-\theta_0)\, H_m(k_0 a) \right) =$$

$$-\rho_1 \sum_{m=o}^{\infty} B_m \cos m(\theta-\theta_0)\, J_m(k_1 a) \qquad 5b)$$

2. Normal velocity continuity

$$\frac{\partial \Phi_{in}}{\partial r} + \frac{\partial \Phi_{sc}}{\partial r} = \frac{\partial \Phi_{tr}}{\partial r} \qquad \text{at } r=a \qquad 6a)$$

$$\frac{-iQ_0 k_0}{4} \sum_{m=o}^{\infty} \varepsilon_m \cos m(\theta-\theta_0) H_m(k_0 S) J_m'(k_0 a)$$

$$+ k_0 \sum_{m=o}^{\infty} A_m \cos m(\theta-\theta_0) H_m'(k_0 a) =$$

$$k_1 \sum_{m=o}^{\infty} B_m \cos m(\theta-\theta_0) J_m'(k_1 a) \qquad 6b)$$

where the prime denotes differentiation with respect to the argument.

The solution for the total (incident plus scattered) acoustic velocity potential is the far field ($r > S$) is, thus:

$$\Phi_T = \frac{-iQ_0}{4} e^{-i\omega t} \left\{ \sum \varepsilon_m \cos m(\Theta-\theta_0) H_m(k_0 r) \left[J_m(k_0 S) - \frac{H_m(k_0 S) \left(\frac{c_1}{c_0} J_m'(k_0 a) J_m(k_1 a) - \frac{\rho_0}{\rho_1} J_m(k_0 a) J_m'(k_1 a)\right)}{\frac{c_1}{c_0} H_m'(k_0 a) J_m(k_1 a) - \frac{\rho_0}{\rho_1} H_m(k_0 a) J_m'(k_1 a)} \right] \right\} \quad 7)$$

As a check, when $\rho_1 >> \rho_0$ (flow cylinder approaches a rigid cylinder) and $S >> a$ (incident wave approaches a plane wave), the scattered wave portion of expression 7 reduces to the solution for the wave scattered from a plane wave incident on a solid cylinder, as given in section 8.1 of reference 5.

III RESULTS

The total sound pressure is evaluated from the acoustic velocity potential by:

$$P_T = -\rho_0 \frac{\partial \Phi_T}{\partial t}$$

The total sound pressure is normalized by the incident sound pressure. The magnitude of this ratio is plotted against variations in frequency, source jet-spacing and angle.

A. Frequency and Spacing Distribution

Figure 2 is the plot of normalized sound pressure against the wave number normalized by the jet radius, $k_0 a$. Included in the figure are plots for values of source/jet-spacing : $S/D = 1.00, 2.667, 5.00$; where D is the jet diameter. The receiver is located at $(\Theta-\Theta_0) = \pi$, or the receiver is on the side of the jet opposite the source.

At low frequencies, $k_o a << 1$ the normalized pressure approaches 1., indicating that the source noise diffracts around the jet. As frequency increases, the normalized pressure decreases to a minimum value. This is the shielding zone in which the jet acts as a partial noise barrier. Above the frequency of minimum sound pressure, the normalized pressure increases rapidly to a terminal value which fluctuates between 0.4 and 0.7.

The effect of increasing the spacing between the source and the jet is to shift the curve to higher frequencies. As the spacing increases, the jet becomes a less efficient barrier because more of the incident sound energy diffracts around the jet into the shadow zone.

These results compare favorably with experimental results by Kantola (6). The data show a rapid increase in source noise shielding beginning at $k_o a \approx .35$. The noise reduction reaches a maximum at values of the wavenumber $1.7 < k_o a < 3.5$, after which the shielding fluctuates about a terminal value less than the maximum. The data show that variation of the source-shielding jet separation shifts the curves along the frequency axis. Kantola's results indicate that an increase in spacing shifts the curve to lower frequencies, which result is not consistent with the trend shown in Figure 2.

The curves in Figure 2 are further normalized by a term involving the ratio of the spacing, S, and the jet diameter D. The results are shown in Figure 3, where the normalized pressure is plotted against $(k_o a)(\frac{S}{D})^{-.2}$. This normalization collapses the curves for the frequencies near the onset of shielding, which occurs at the value of the normalized frequency of 0.175, and at frequencies above the minimum normalized pressure. Near the minimum normalized pressure, the analytical functions are not well behaved. However, the trend of the curves indicate that the maximum shielding occurs at the normalized frequency parameter of 2.72. No clear trend is exhibited for the minimum normalized pressure as a function of spacing. The minimum value ranges between 0.22 and 0.42.

B. Azimuthal Distribution

Figures 4 and 5 demonstrate the variation of normalized pressure in the plane normal to the axis of the shielding jet. Figure 4 is for S/D = 1.0 and Figure 5 is for S/D = 2.667. Because of symmetry, only the half plane is shown. The normalized pressure is evaluated at points on a circle which is centered on the noise source.

All plots shown indicate that the normalized pressure is approximately 1. at $\alpha = 90°$, or off to the side of the source. This result is consistent with measured data (7,8).

At frequencies near the onset of shielding, $(k_o a)(\frac{S}{D})^{-.2} \approx 0.2$, the distribution of the sound pressure is uniform around the shielding jet, and the incident sound is not influenced by the jet's presence. At frequencies between the onset of shielding and the maximum shielding, $0.2 < (k_o a)(\frac{S}{D})^{-.2} < 2.72$, the incident sound energy is scattered into two major lobes, one back toward the noise source and the other on the side of the jet opposite the source. As the maximum shielding is approached, the scattered energy becomes concentrated into the lobe on the side of the jet opposite the source, with no scattering back toward the source.

The shadow zone, the region on the side of the jet opposite the source in which the normalized pressure is less than 1.0; becomes narrower and the attenuation greater as the frequency is increased. Comparing Figures 4 and 5, the shadow zone becomes narrower as the jet spacing increases.

The included angle β, is the angle within which the normalized pressure is less than 1.0. This angle is plotted in Figure 6 against the product of the wavenumber and the jet spacing. The relationship for β is found to be:

$$\beta = 2.20\ (k_o S)^{-.37} \qquad 8)$$

where β is expressed in radians.

The angle β thus defines the width of the jet shielding zone. For a given wavenumber and spacing between the source and the jet, shielding is expected to occur at values of β less than that calculated from expression 8. The sound pressure increases rapidly, however, at values of β greater than the calculated value, as seen by the lobes to the side of the shielding zone in Figures 4 and 5.

IV SUMMARY

The two-dimensioned wave equations have been solved to estimate the diffraction and reflection of sound by a heated, cylindrical jet. The sound pressure is evaluated on the side of the jet opposite the source, where shielding is expected to be a maximum. The results show that the sound pressure decreases rapidly with frequency beyond the onset of the shielding to a minimum value. At frequencies greater than those for which the sound pressure is a minimum, the sound pressure approaches a terminal value, which is greater than the minimum. This trend is expected form barrier theory and is consistent with the experimental results. The results also show that increasing the spacing between the source and the jet shifts the curves toward higher frequencies. This result is expected from barrier considerations but is not confirmed by available experimental data.

The azimuthal distribution of the sound of the sound pressure shows that as the frequency increases from the onset of shielding to the frequency at which maximum occurs; the amount of back scattering decreases and scattered energy becomes more highly concentrated in lobes to the sides of the shadow zone. The shadow zone becomes narrower as the spacing is increased.

The two-dimensional model, while a simplification of the twin jet shielding phenomenon, is useful in demonstrating expected trends. Development of the model in three-dimensions is currently underway. With this three-dimensional model , the phenomena of forward and back scattering along the jet axis can be investigated as well as the effects on shielding of mach number.

This work is supported by NASA Langley, Acoustics and Noise Reduction Division.

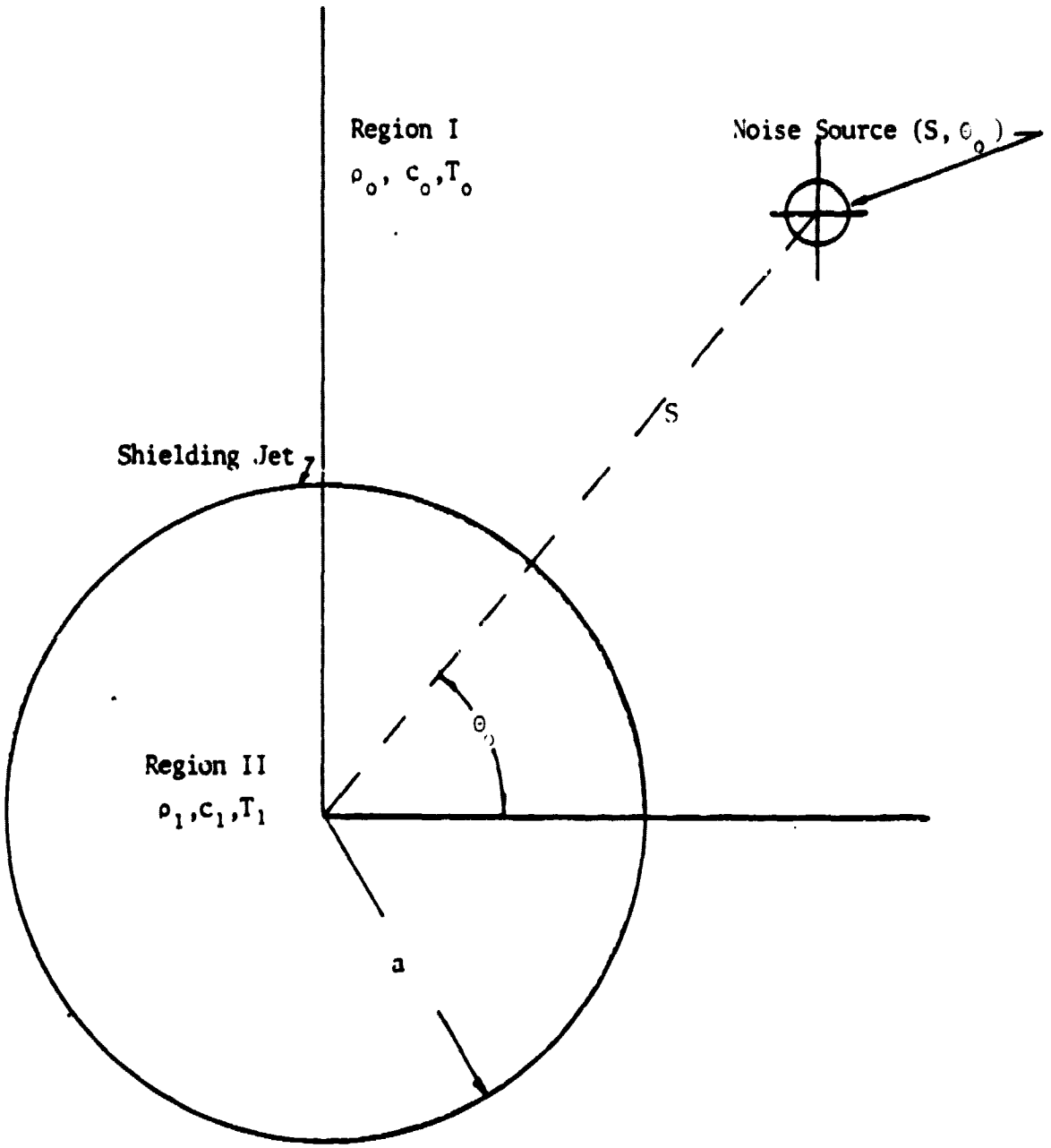

Figure 1: Noise-source/Shielding Jet Geometry for Jet Shielding Analysis

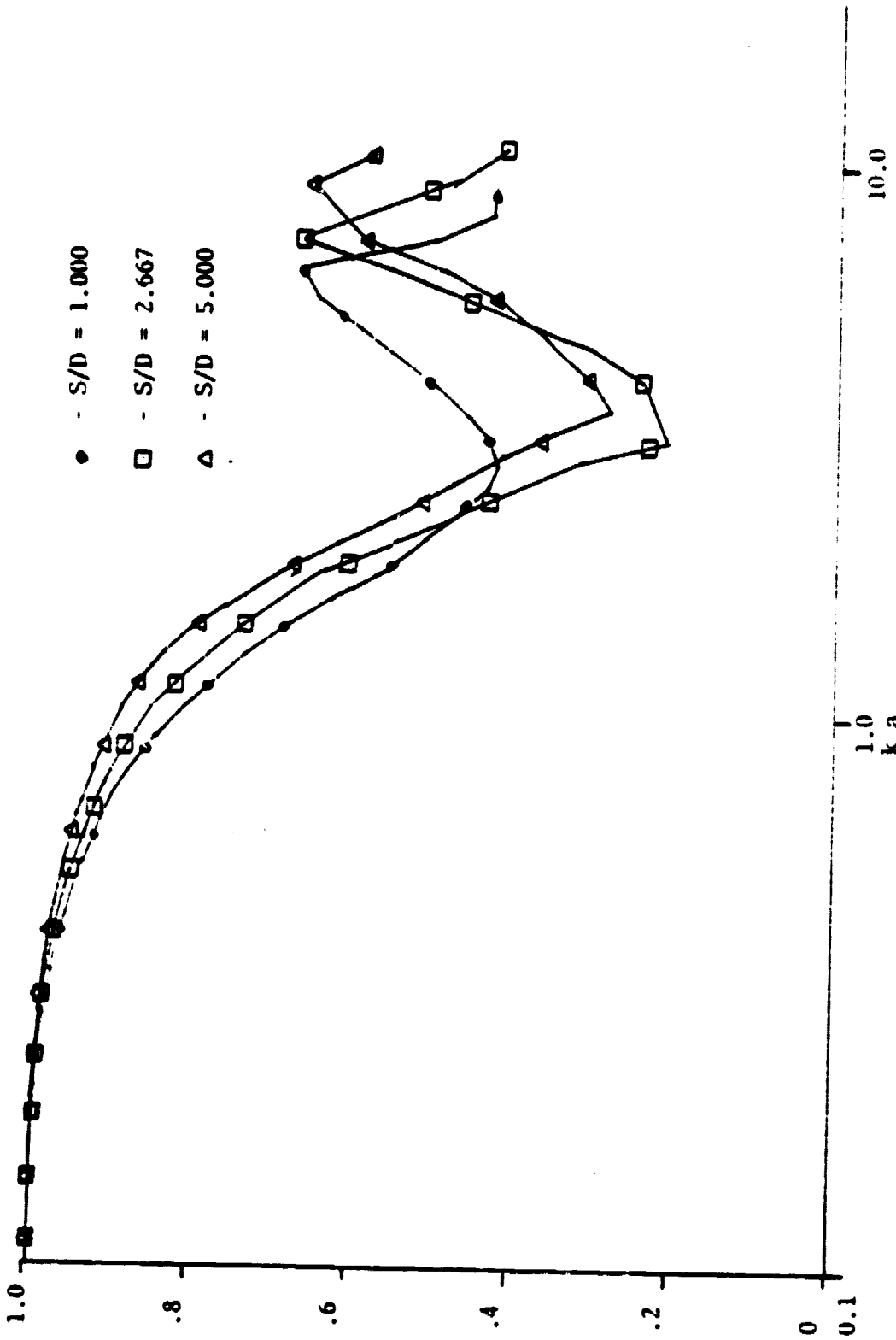

Figure 2: Normalized Sound Pressure vs. Wavenumber x Jet Diameter, Various Jet Spacings

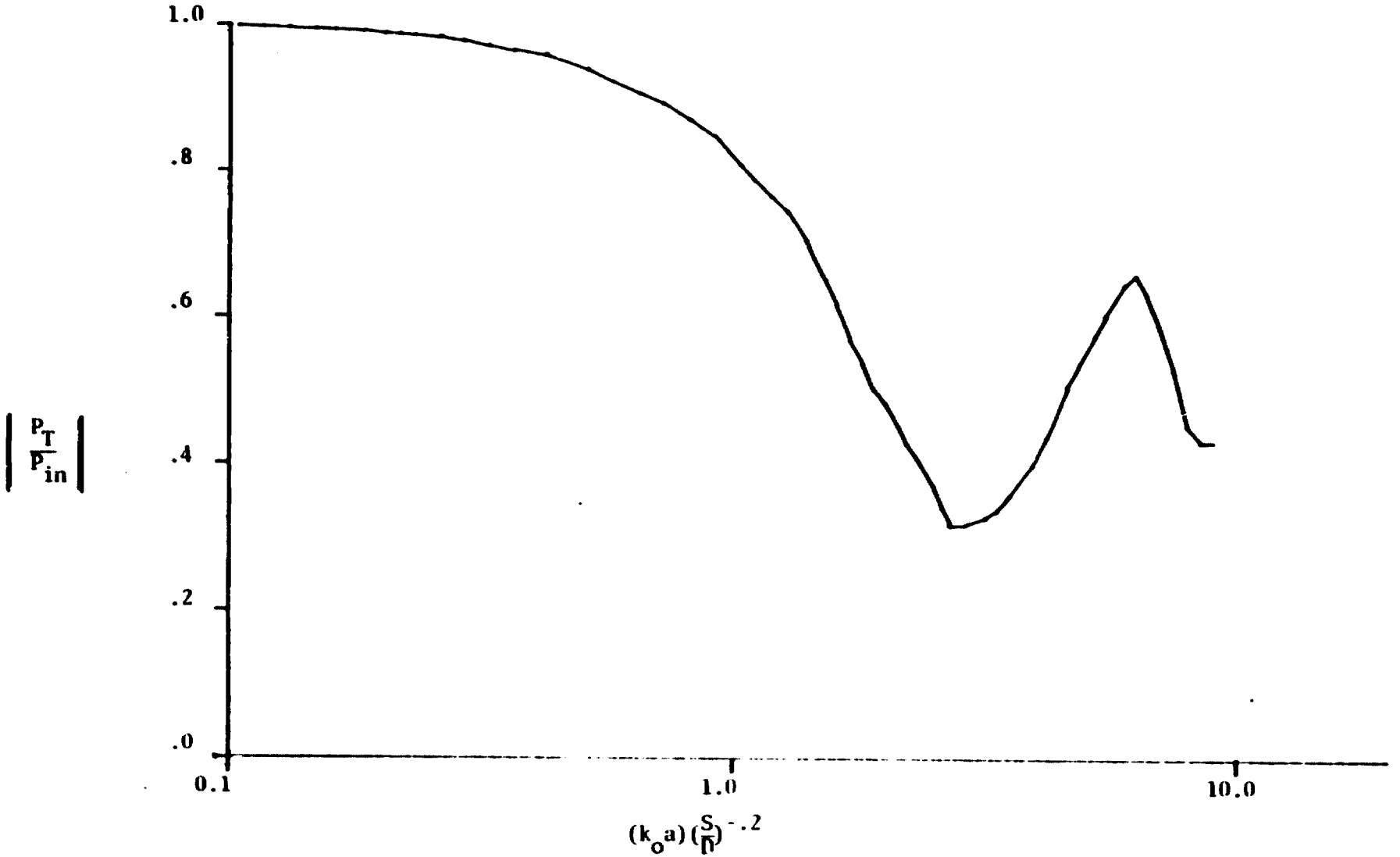

Figure 3: Normalized Sound Pressure vs. Normalized Frequency Parameter, all Jet Spacings

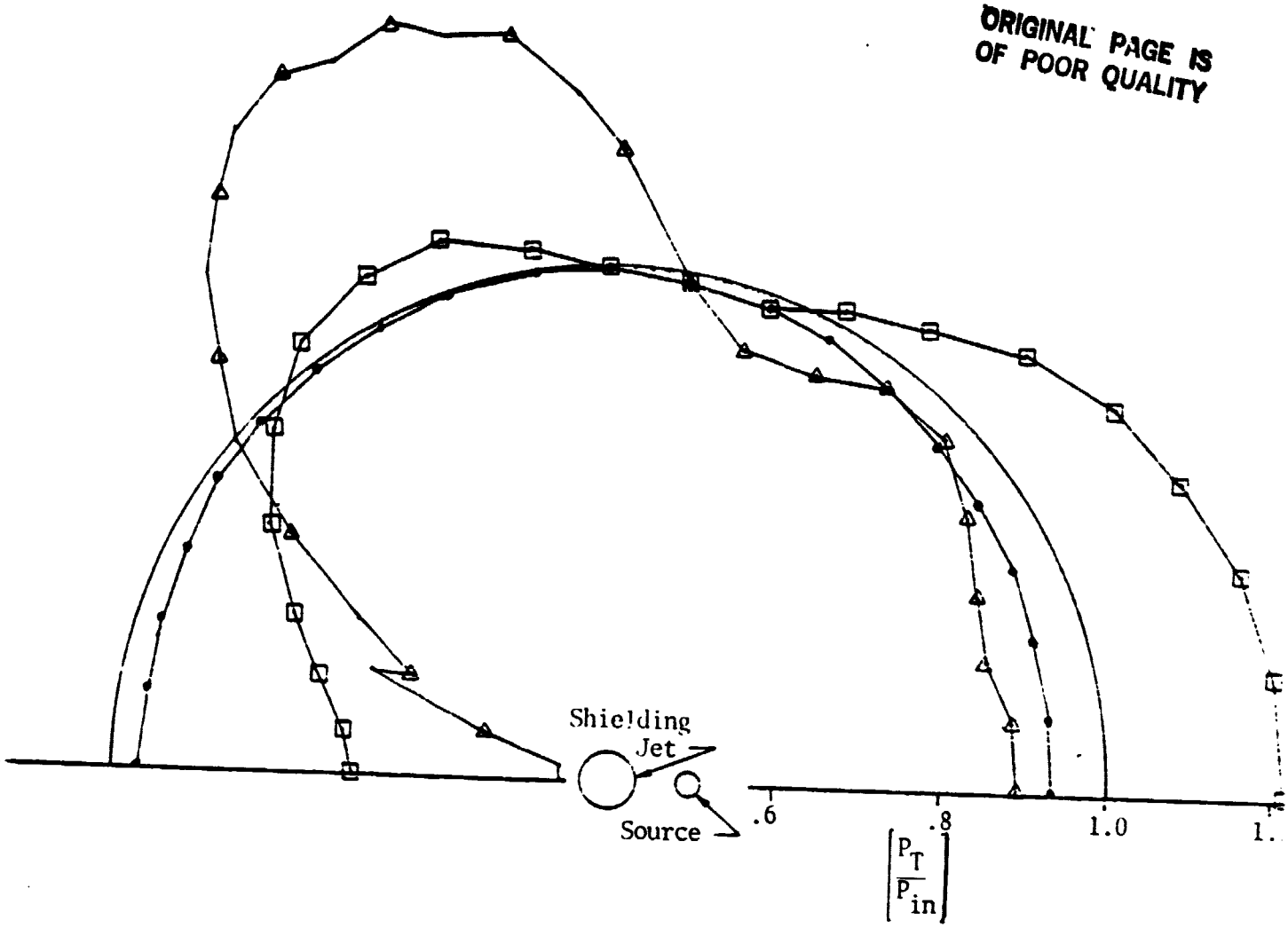

Figure 4: Normalized Pressure vs. Azimuthal Angle Around Noise Source, half-plane shown. S/D = 1.000

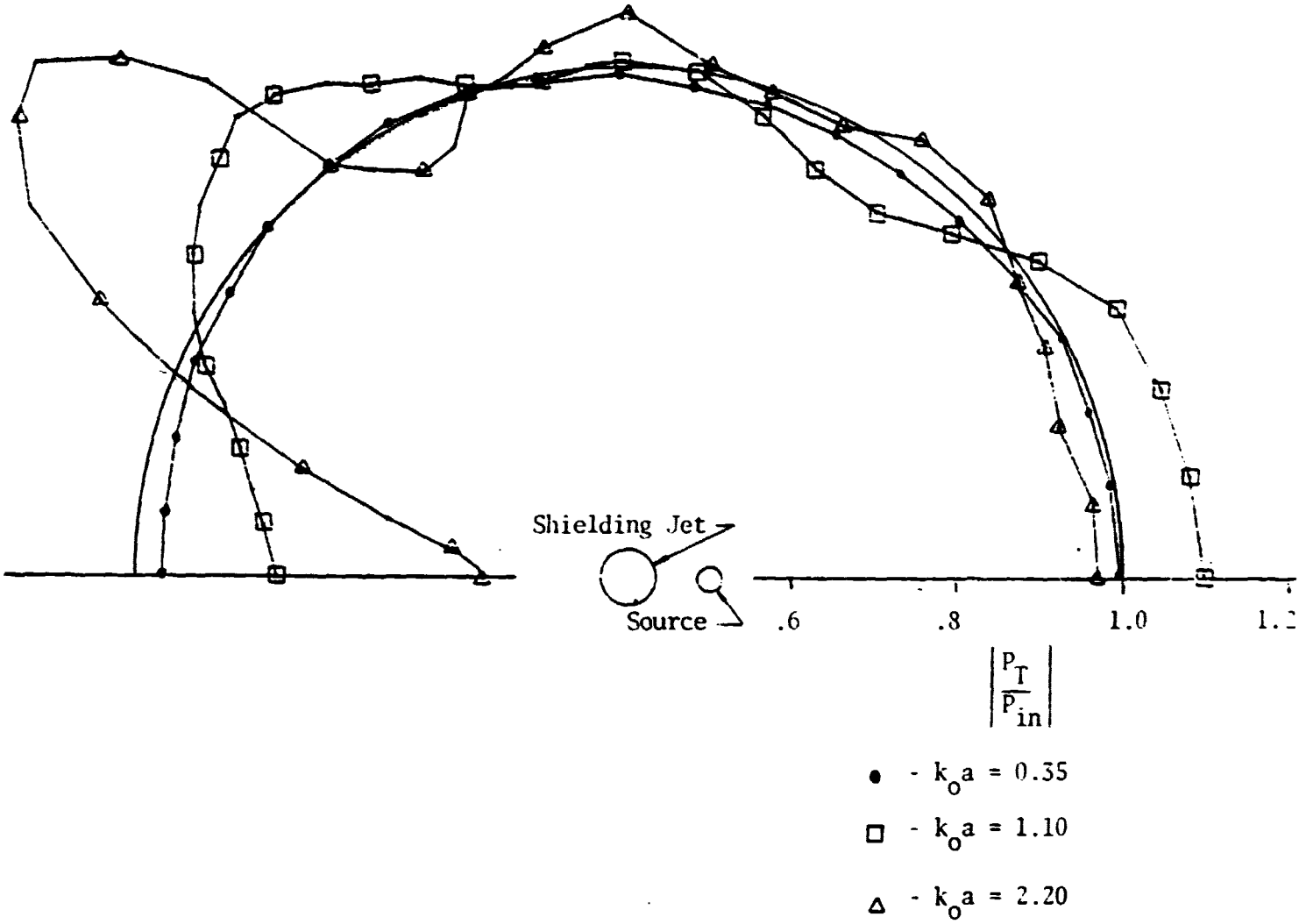

Figure 5: Normalized Pressure vs. Azimuthal Angle Around Noise Source, half-plane S/D = 2.667

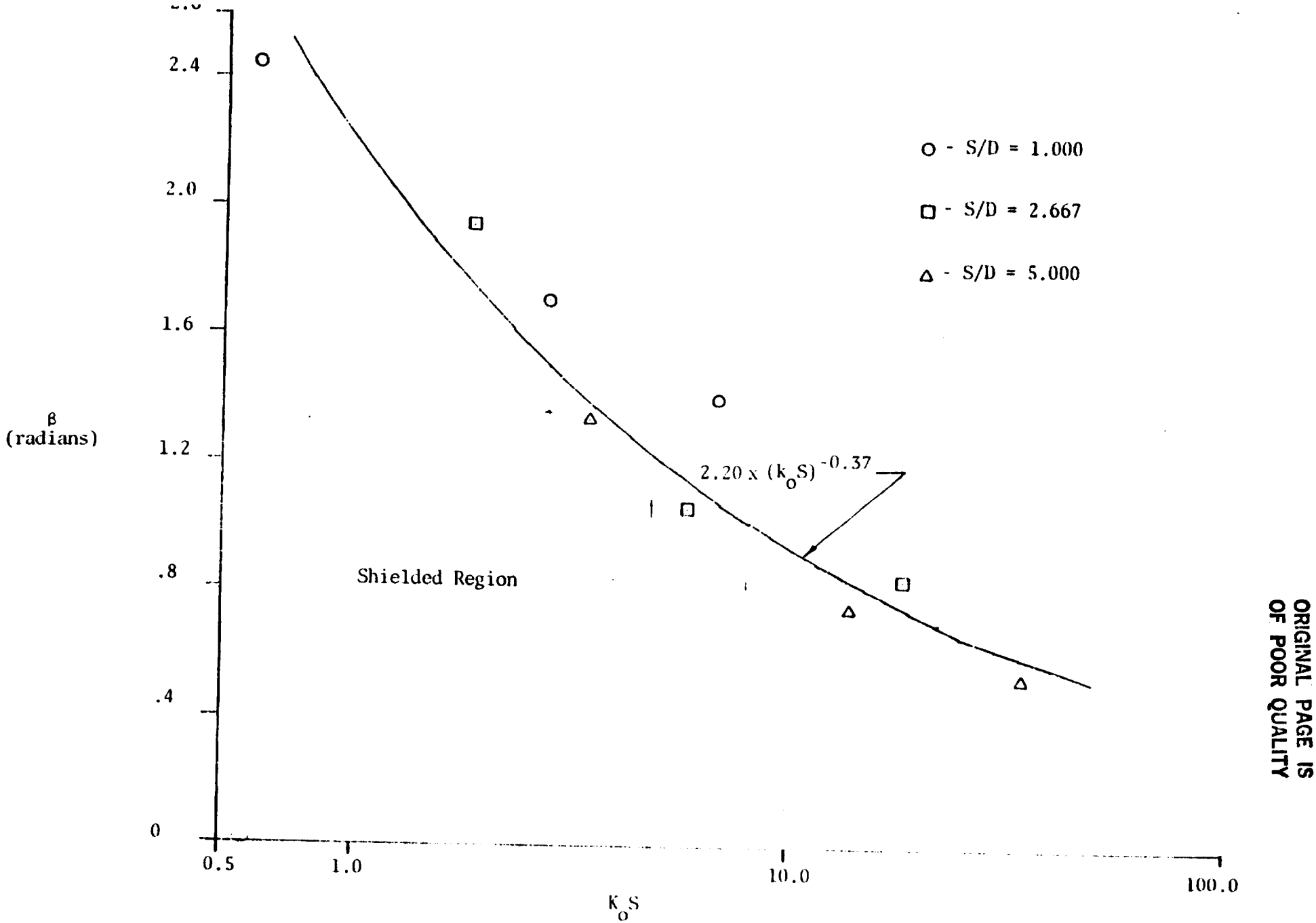

Figure 6: Included angle at which the Normalized Pressure is 1.0. Defines Width of Jet Shielding Zone.

REFERENCES

1) Ribner, H.S., "Reflection, Transmission, and Amplification of Sound by a Moving Medium", JASA vol. 29, no 4, p.435

2) Miles, J.W., "On the Reflection of Sound at an Interface of Relative Motion", JASA vol. 29, no 2, p.226

3) Yeh, C., "Reflection and Transmission of Sound Waves by a Moving Fluid Layer", JASA vol. 41, no. 4, p.817

4) Yeh, C., "A Further Note on the Reflection and Transmission of Sound Waves by a Moving Fluid Layer", JASA vol. 43, no. 6, p. 1454

5) Morse, P. and Ingard, P., Theoretical Acoustics", McGraw-Hill, 1968

6) Kantola, R.A., "Shielding Aspects of Heated Twin Jet Noise" Presented at the AIAA 4th Aeroacoustics Conference. Atlanta, Georgia. Oct. 3-5, 1977

7) Parthasarathy, S.P., Cuffel, R.F., and Massier, P.F., "Twin Jet Study, Final Report". Jet Propulsion Laboratory, California Institute of Technology, Pasadena, California. Nov.3, 1978